Behavioral/Cognitive

Selective Enhancement of Post-Sleep Visual Motion Perception by Repetitive Tactile Stimulation during Sleep

Yoshiyuki Onuki,[1] Oti Lakbila-Kamal,[1] Bo Scheffer,[1] Eus J. W. Van Someren,[1,2,3] and Ysbrand D. Van der Werf[4]
[1]Department of Sleep and Cognition, Netherlands Institute for Neuroscience, an institute of the Royal Netherlands Academy of Arts and Sciences, Amsterdam, 1105BA, The Netherlands, [2]Department of Integrative Neurophysiology, Center for Neurogenomics and Cognitive Research, Amsterdam Neuroscience, VU University Amsterdam, Amsterdam, 1081HV, The Netherlands, [3]Amsterdam UMC, Vrije Universiteit, Psychiatry, Amsterdam Neuroscience, Amsterdam, 1081HV, The Netherlands, and [4]Department of Anatomy and Neurosciences, Amsterdam UMC, location VU, University Medical Center, Amsterdam, 1081HZ, The Netherlands

Tactile sensations can bias visual perception in the awake state while visual sensitivity is known to be facilitated by sleep. It remains unknown, however, whether the tactile sensation during sleep can bias the visual improvement after sleep. Here, we performed nap experiments in human participants ($n = 56$, 18 males, 38 females) to demonstrate that repetitive tactile motion stimulation on the fingertip during slow wave sleep selectively enhanced subsequent visual motion detection. The visual improvement was associated with slow wave activity. The high activation at the high beta frequency was found in the occipital electrodes after the tactile motion stimulation during sleep, indicating a visual-tactile cross-modal interaction during sleep. Furthermore, a second experiment ($n = 14$, 14 females) to examine whether a hand- or head-centered coordination is dominant for the interpretation of tactile motion direction showed that the biasing effect on visual improvement occurs according to the hand-centered coordination. These results suggest that tactile information can be interpreted during sleep, and can induce the selective improvement of post-sleep visual motion detection.

Key words: **consolidation; cross-modal interaction; sleep; tactile; vision**

Significance Statement

Tactile sensations can bias our visual perception as a form of cross-modal interaction. However, it was reported only in the awake state. Here we show that repetitive directional tactile motion stimulation on the fingertip during slow wave sleep selectively enhanced subsequent visual motion perception. Moreover, the visual improvement was positively associated with sleep slow wave activity. The tactile motion stimulation during slow wave activity increased the activation at the high beta frequency over the occipital electrodes. The visual improvement occurred in agreement with a hand-centered reference frame. These results suggest that our sleeping brain can interpret tactile information based on a hand-centered reference frame, which can cause the sleep-dependent improvement of visual motion detection.

Introduction

Tactile sensory information, such as texture and hardness, influence our visual information by way of cross-modal interaction. For instance, tactile sensory inputs can strengthen visual motion perception when the two modalities are presented congruently in a direction-sensitive manner (Bensmaïa et al., 2006). However, when visual and tactile stimuli are presented with a delay, repeated exposure to tactile motion stimulation produces a counterphase motion aftereffect in the visual modality afterward (Konkle et al., 2009; Xiao et al., 2021). The presumed neural mechanism underlying this cross-modal interaction relies on processing in partially overlapping neural circuits. For example, the primary visual cortex and human middle temporal/V5 complex (hMT/V5) show activation during the tactile orientation processing and tactile motion processing (Zangaladze et al., 1999; Hagen et al., 2002). In addition, the primary somatosensory cortex (S1) shows directionally selective neural responses to both visual and tactile motion stimulations (Pei et al., 2010; Pei and Bensmaia, 2014). The above-mentioned evidence suggests that the tactile sensory inputs can act to both facilitate, and adapt

Received July 23, 2021; revised May 7, 2022; accepted June 12, 2022.

Author contributions: Y.O., E.J.W.V.S., and Y.D.V.d.W. designed the experiments; Y.O. O.L.-K., and B.S. collected the data; Y.O., O.L.-K., and B.S. analyzed the data and performed sleep scoring; Y.O., E.J.W.V.S., and Y.D.V.d.W. wrote the manuscript.

This work was supported by the Programmes for Excellence "Brain & Cognition: an Integrated Approach", 433-09-245. We thank Joris Coppens for building the MR compatible tactile stimulus delivery device, Mike X. Cohen for advices on EEG analysis, Jennifer R. Ramautar and Germán Gómez-Herrero for technical assistance in the sleep experiments, Verena Sommer for technical assistance in the preliminary experiments, Chris I. de Zeeuw, Ryo Kitada, and Astrid M.L Kappers for the helpful comments on the results.

Y. Onuki's present address: Department of Neurosurgery, Jichi Medical University, Tochigi, 329-0498, Japan.

The authors declare no competing financial interests.

Correspondence should be addressed to Ysbrand D. Van der Werf at yd.vanderwerf@amsterdamumc.nl or Yoshiyuki Onuki at y.onuki@jichi.ac.jp.

https://doi.org/10.1523/JNEUROSCI.1512-21.2022

to, visual motion processing through the shared neural circuits between the visual and tactile domains. To date, most studies have focused on visual and tactile cross-modal interactions during the awake state, but no research has assessed these interactions during sleep.

Sleep plays an important role to facilitate our visual system, for instance in the form of visual perceptual learning, that is, the visual enhancement through practices, such as texture discrimination and motion discrimination (Mednick et al., 2003; Sasaki et al., 2010), and even perceptual exposure of the task-irrelevant visual motion stimulus (Watanabe et al., 2001). The visual improvements after sleep correlate with the extent of activation of the trained visual cortical region (Yotsumoto et al., 2009) and with slow wave initiation during sleep (Mascetti et al., 2013). The role of sleep in the facilitation of visual perception and the interaction between the visual and tactile modalities suggest that the tactile motion stimulation during slow wave sleep could improve the visual motion detection in a direction-selective manner: either in the direction of the presented tactile stimulation or in the direction opposite to the tactile motion because of adaptation.

Furthermore, in the awake state, tactile spatial perception is attributed to the integration of information weights assigned to multiple spatial reference frames, such as hand/skin, head, and vision (Heed et al., 2015). The context of the task demand modulates the weights to adjust the tactile spatial processing via a top-down signal (Azañón and Soto-Faraco, 2008). Previous studies have shown that, with closed eyes, as it happens during sleep, either a hand- or head-centered reference frame (an alternative of a world-centered reference frame) can potentially underlie tactile direction-selective effects (Carter et al., 2008; Moscatelli et al., 2015). However, the specific body reference frame contributing to possible behavioral improvements through visual-tactile interaction during sleep remains unknown.

The present study addressed whether visual-tactile cross-modal interactions during sleep affect the subsequent wake performance. First, we examined the performance changes in the visual motion detection across sleep and wakefulness periods with tactile motion stimulation to the index finger using a 64-pin braille-type tactile device. A custom-built closed-loop interface was used to target directional tactile stimulation to the finger based on the detection of the amplitude features of the sleep slow waves from an EEG. Next, using the same closed-loop interface, we performed directional stimulation in a new group of participants sleeping with their arms outstretched to create a misalignment situation with multiple body reference frames, thereby allowing us to observe whether behavioral improvements depend on a head- or hand-centered reference frame.

Materials and Methods

Participants

In Experiment 1, 83 right-handed healthy participants who passed the online questionnaire were recruited for the sleep experiment. Twenty-seven participants were excluded from the analysis for the following reasons: awareness of the direction of the tactile motion stimulation during sleep ($n = 1$), an insufficient number (10 times) of tactile stimulations presented in sleep Stage N3 ($n = 10$), accidental detachment of index finger from the tactile stimulation device owing to spontaneous body movements in sleep ($n = 4$), technical failure of the closed-loop interface ($n = 8$), or excessive response bias (i.e., $\geqq$ 100 times) toward one of the eight response options during the visual motion task because of fatigue ($n = 4$). Accordingly, the remaining 56 participants were included in the analysis (18 males, 38 females, 23.0 $\pm$ 0.47 [mean $\pm$ SEM] years old). In Experiment 2, 38 participants who passed the online questionnaire but did not participate in Experiment 1 were recruited for the experiment. Fourteen participants (14 female, 22 $\pm$ 0.99 [mean $\pm$ SEM] years old) were included in the analysis. Twenty-four participants were excluded from the analysis because of shallow sleep ($n = 13$), awareness of the direction of the tactile motion stimulation during sleep ($n = 2$), excessive response bias (i.e., $\geqq$ 100 times) toward one of the eight response options during the visual motion task because of fatigue ($n = 3$), an insufficient number (i.e., $\leqq$ 10 times) of tactile stimulations presented in sleep Stage N3 ($n = 2$), technical failure of the closed-loop interface ($n = 1$), accidental detachment of index finger from the tactile device ($n = 1$), and changing arm position because of body movements during sleep ($n = 2$). All participants followed the same instruction used in Experiment 1. The number of participants is determined based on sample sizes referring to prior sleep studies of the targeted memory enhancement (Rasch et al., 2007; Rudoy et al., 2009; Antony et al., 2012).

The protocol of the experiment was approved by the ethics committee of the Department of Psychology, University of Amsterdam. All participants signed a consent form before the experiment. None of the participants had a history of excessive intake of alcohol and/or drugs, neurologic, psychological, sleep or sensory disorders, or medication use that may affect cognitive function.

Online questionnaire and sleep quality check before the experiment

All participants were examined by an online questionnaire before their recruitment as participants. The online questionnaire consisted of questions regarding medication and current or prior diagnoses of neurologic or psychiatric disorders, the Athens Insomnia Scale (Soldatos et al., 2000), Pittsburgh Sleep Quality Index (Buysse et al., 1989), and Ford Insomnia Response to Stress Test (Chang et al., 1997). All selected participants scored below the cutoff for insomnia or other sleep disorders (Pittsburgh Sleep Quality Index < 5, Athens Insomnia Scale < 6) and stress responsivity (Ford Insomnia Response to Stress Test < 19).

To verify regular sleep cycles 3 d before the experiment, wrist movements were recorded using an actigraph (GENEActiv, Activeinsights). During actigraphy, participants were instructed to keep a sleep diary (Carney et al., 2012). All participants slept $>$7 h daily and maintained their regular bedtimes in the days preceding the experiment. The participants were instructed to refrain from any intake of caffeine and medicine for 24 h before the sleep experiment.

Experimental design

The experiment was conducted in a soundproof bedroom of the sleep laboratory at the Department of Sleep and Cognition, The Netherlands Institute for Neuroscience. The behavior of each participant during the experiment was monitored by an infrared video camera (IPELA, Sony). The experiment was held from 10:30 A.M. to 3:30 P.M. to keep the same experimental schedule across participants, thereby avoiding the effects of circadian rhythm on cognitive performance (time-of-day effects). Participants were randomly assigned to one of sleep/wake conditions (SLEEP-MOTION, SLEEP-RANDOM, and WAKE-MOTION conditions, Fig. 1*A*). Each condition consisted of 14 participants.

In Experiment 1, the pre-test session of the visual motion task was conducted from 10:30 A.M. to 11:30 A.M., after the assessment sessions to determine the motion coherence threshold for the pre-test task.

Following the 30 min lunch intermission, there was 60 min preparation of the polysomnography, including EEG, EOG, and chin EMG for the sleep conditions (SLEEP-MOTION and SLEEP-RANDOM conditions). The sleep session in all sleep conditions or rest session in the WAKE-MOTION condition took place from 1:00 P.M. to 2:30 P.M. In the sleep session, participants lay down on the bed and received tactile motion stimulation of one of four directions (up, down, left, right) in the SLEEP-MOTION condition or tactile random stimulation during slow wave activities mainly in sleep N3 sleep. The tactile device was placed under a thick blanket to avoid any sounds from the stimulation device potentially disturbing the participants' sleep. In the SLEEP-MOTION and SLEEP-RANDOM conditions, the participants who only entered light sleep (Stage N1-N2) without receiving tactile stimulation were recategorized as the LIGHT SLEEP–NO STIMULATION condition. In the rest session for the WAKE-MOTION condition, participants sat upright behind a desk and received one of four tactile motion

stimulation used in SLEEP-MOTION conditions from the device on the tabletop, following the previous study of visual-tactile motion perception (Konkle et al., 2009). The hand and tactile device were also covered by a small towel.

After the 30 min intermission to recover from sleep inertia for the sleep conditions, the post-test session of the visual motion task was conducted with the same threshold used in the pre-test session. Subsequently, participants filled out the post-experiment questionnaire and the areas of their right index fingertips were measured.

In Experiment 2, participants were assigned to the SLEEP-POSTURE condition. In this condition, participants received the upward linear tactile stimulation used in the SLEEP-MOTION condition. When receiving the tactile stimulation during sleep, their right arms were stretched out in a 90 degree angle away from the body. A small towel was placed under the arm to support the stretched arm. The experimental procedure and time schedule were the same in the SLEEP-MOTION condition of the Experiment 1.

Visual random dot motion task

To quantify the visual motion detection ability in different directions, participants performed the random dot motion task (Shadlen and Newsome, 1996; Watanabe et al., 2001) in the pre-test and post-test sessions (Fig. 1*B*). The stimulus consisted of a subset of dots moving coherently toward one of eight particular directions (0°, 45°, 90°, 135°, 180°, 225°, 270°, and 315° in polar coordinates) within a noise of randomly moving dots. The moving dots were presented for 500 ms after displaying each trial number for 1 s. The dots moved 8°/s and had a density of 0.935 dots/deg^2. The diameter of the stimulation area was 14.6°. The task was programmed in Psychtoolbox 3 (Brainard, 1997) installed in MATLAB (R2011b, The MathWorks). The stimulation was displayed on a gamma-corrected CRT monitor (Dell Trinitron P1130, DELL) under dark conditions. The distance between the computer screen and the eyes of the participants was 43 cm. To keep the same distance across trials and to minimize fatigue during the task, the participant's head was supported by a chin rest (HeadSpot, UHCO Technical Services).

Preceding the pre-test session, assessment sessions were held for 15 min to measure the individual threshold of visible motion coherence level (50% performance level in a two-alternative forced choice task) using a staircase method. After the assessment sessions, participants performed the pre-test session of the random dot motion task with eight possible response options for ~30-40 min. The task consisted of 240 trials with a 1 min intermission after every 48 trials to minimize fatigue during the task. No time restriction was applied for giving the response. No feedback for correct/incorrect responses was provided in both the assessment session and the pre-test/post-test sessions.

Closed-loop interface for automatic slow wave detection and tactile stimulation

To present tactile stimulation to participants during slow wave sleep, we created a closed-loop interface to detect slow wave activities and to present tactile stimulation in real time (Fig. 1*C*,*D*). This interface consisted of the streaming of EEG data, preprocessing, artifact detection, slow wave detection, and tactile stimulation.

The 256-channel EEG data were acquired at 500 Hz sampling frequency using a Geodesic EEG system and Amp server pro SDK (Electrical Geodesics) implemented in Mac Pro (Apple). The acquired data were streamed in chunks of 1024 data points to the EEG processing computer. In the processing computer, the streamed data were imported by BCI2000 (Schalk et al., 2004) and the 3-channel EEG data of the frontal electrode (Fz) and left and right mastoids were used for the further analysis. The streamed EEG data (Fz) were rereferenced by using the average EEG data of the left and right mastoids, detrended, bandpass filtered from 0.5 to 50 Hz, multiplied by a Hanning window, and converted to an amplitude spectrum calculated by the absolute value of the fast Fourier transform (FFT).

The epochs of preprocessed data were analyzed by the artifact detector and slow wave detector. The artifact detector assessed the preprocessed EEG data first; and subsequently, the slow wave detector examined the data that passed the artifact detector.

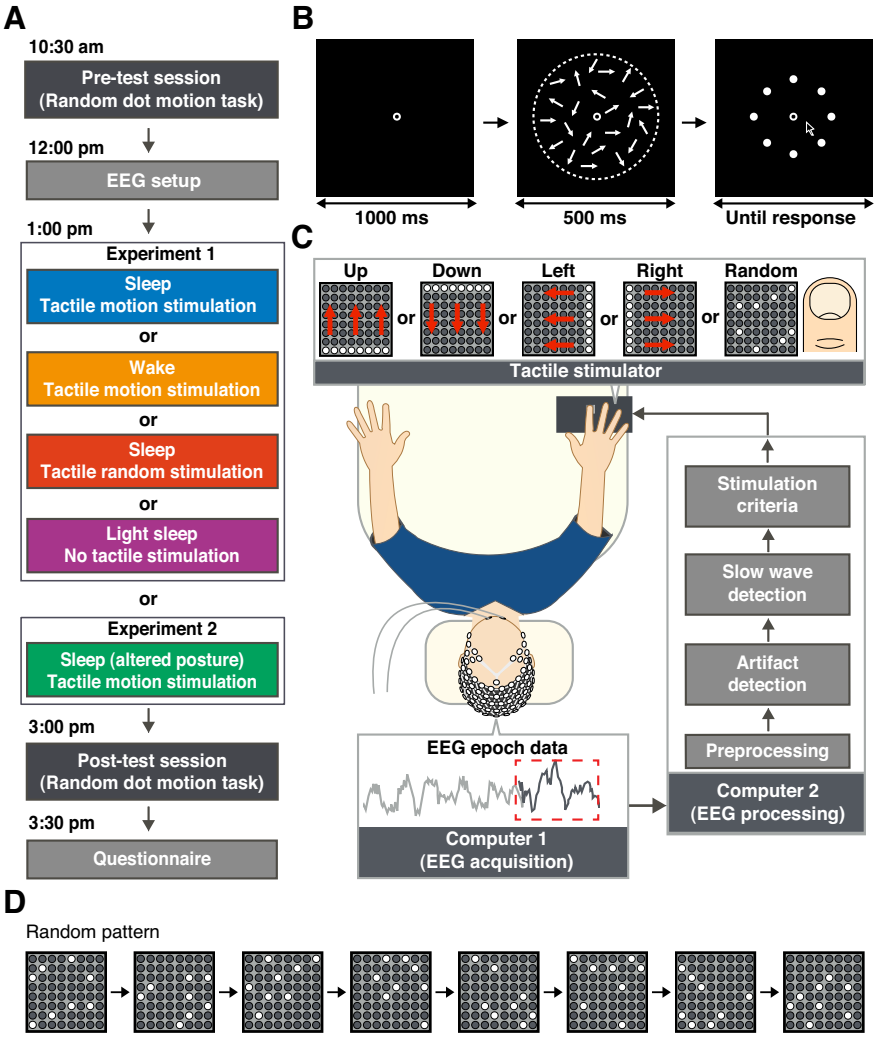

Figure 1. Experimental procedure, the visual motion task, the setup, and tactile stimulation types of the closed-loop interface for the sleep experiment. ***A***, Experimental procedure and timeline. ***B***, The random dot motion task. A fixation screen was followed by an array of moving dots. Subsequently, the subject chose the perceived direction from eight response options (white filled circles) by a mouse click. No tactile stimulation was assigned during the task. The white dot circle was drawn for visualization purposes and not presented during the task. ***C***, The closed-loop interface presented tactile stimulation on the assessments of the artifact and slow wave detectors and the stimulation criteria (a minimum of 15 slow waves in the preceding minute). In the tactile motion stimulation conditions, 8 adjacent white plastic pins forming a line popped up simultaneously for 25 ms and moved in one of four directions (up, down, left, right) to establish the sensation of a linear movement. In the tactile random stimulation, every plastic pin popped up once per stimulation, thus stimulating the entire index fingertip and maintaining the same spatial-temporal features between both stimulation types, except the motion feature. ***D***, An example of the tactile random stimulation.

The tactile stimulation was performed on the right index fingertip from the custom-made tactile device when the slow wave detector classified EEG epochs as the slow wave activity >15 times in the preceding 60 s. The distal and proximal interphalangeal joints of the index finger were taped on the tactile device to maintain the same position on the active area of the instrument during the sleep experiment. A gel mousepad was placed under the palm and wrist of the right hand to support the hand.

Construction of artifact and slow wave detectors

To construct the detectors of movement artifact and slow wave activity, we used a machine-learning algorithm, the Support Vector Machine with the radial-basis-function kernel, implemented in the LIBSVM toolbox (Chang and Lin, 2011).

All datasets were generated from 90 min sleep EEG data of a total of 15 participants of other sleep experiments conducted in the sleep laboratory of the Department of Sleep and Cognition, The Netherlands Institute for Neuroscience. The sleep data were recorded using the same 256-channel high-density EEG at 500 Hz sampling frequency. None of the participants or sleep scorers of the datasets was involved in this experiment. All datasets were preprocessed in the same manner as the real-time preprocessing. For the construction of the slow wave detector, datasets of 12 participants were used. The training datasets consisted of the concatenated data of the Stage W (Wake) and light sleep (Stages N1 and N2), and the data of Stage N3. A total 1008 epochs of 1024 data points were generated from each participant's data. For the construction of the artifact detector, datasets of breathing and movement artifacts from 12 participants (9 participants' data used for training slow wave detector and 3 additional participants' data) were used. The training datasets consisted of the artifact data and the concatenated data of Stage W and sleep Stages N1, N2, and N3. The 38 epochs of 1024 data points were generated from each participant's data. All data were extracted from the frontal electrode (Fz) after being rereferenced by the averaged EEG data of the left and right mastoid, detrended, bandpass filtered from 0.5 to 50 Hz, multiplied by a Hanning window, and converted to an amplitude spectrum calculated by the absolute value of FFT.

The prediction accuracies of each detector were evaluated by a leave-one-subject-out cross-validation (Fig. 2). The 12 cross-validation datasets were generated; the 11 participant datasets were used to train the detectors, and the remaining one was used to test the detectors. This procedure was repeated 12 times by changing data to validate the accuracies of each detector. Two-sided binomial tests were performed to check the classification performance. To evaluate the accuracies of the detectors in the cross-validation, we drew the receiver operating characteristic curve by shifting the detection threshold of the output probability estimates from the support vector machine and calculated area under the curve (AUC).

Tactile stimulation and stimulation criteria

Tactile stimulation was presented to the right index fingertip on a custom-made MR-compatible tactile stimulator (950 mm height × 1920 mm width × 280 mm depth) in the sleep or rest session. The tactile stimulator consisted of eight piezoelectric actuators (Braille cell B11, Metec AG) to form the 8 × 8 active plastic pin area (21 mm height × 21 mm width) with 64 stimulation spaces (2.45 mm height × 2.45 mm width). Each pin is pushed up 0.7 mm by the actuator and can be operated independently by MATLAB (R2011b, The MathWorks).

For both SLEEP-MOTION and WAKE-MOTION conditions, adjacent linear stimulation of eight pins was presented eight times at 25 ms each to achieve the 200 ms motion sensation. For the SLEEP-RANDOM condition, eight consecutive stimulations that consisted of eight pins chosen randomly were presented with the same parameters as the linear motion stimulation. It ensured that each pin would provide stimulation only once every 200 ms and the total surface area covered in each stimulation cycle was identical between all stimulation types.

For the delivery of the tactile motion stimulation in the sleep or rest sessions of all SLEEP- and WAKE-MOTION conditions, one of four possible directions (up, down, left, right) was selected by the criteria based on the score of the random dot motion task in the pre-test session; the selected direction should be visually perceived at more than chance level (12.5% in an eight-alternative forced choice task) and could not be the most frequently selected direction to avoid the incidental facilitation of the participants' response preferences instead of the facilitation of the visual motion detection ability. The numbers of each motion direction assigned to participants in the SLEEP-MOTION condition were four up, one down, four left, and five right, whereas those of the WAKE-MOTION condition were four up, three down, four left, and three right.

To equalize the interstimulus intervals of the tactile stimulation in the WAKE-MOTION condition with those of the SLEEP-MOTION and SLEEP-RANDOM conditions, we generated a dataset of interstimulus intervals from the kernel probability distribution that was fitted to data within 95th percentiles of the distributions of interstimulation intervals in both sleep conditions. The data generation was performed by the MATLAB function called "fitdist" in the MATLAB statistics toolbox (The MathWorks).

Offline sleep scoring

To qualify the sleep state, the 90 min polysomnographic data recorded in the sleep sessions were scored every 30 s by two well-trained sleep scorers, following the standardized sleep score manual (Iber et al., 2007).

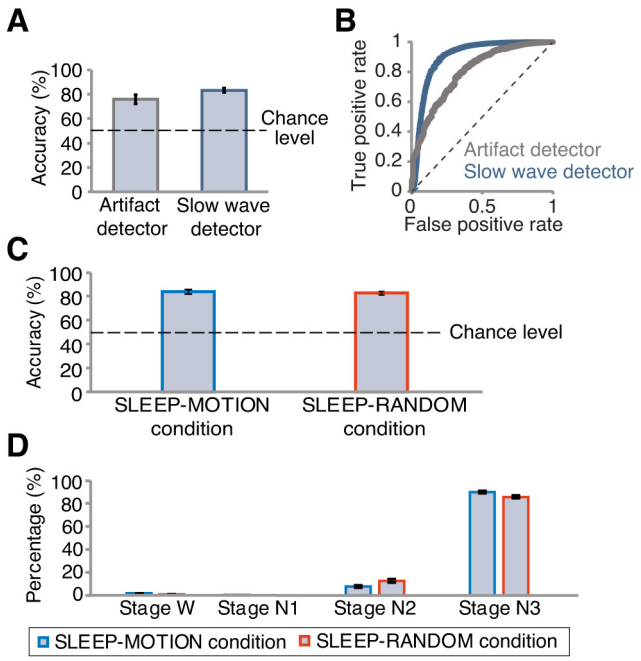

Figure 2. Performance of the artifact and slow wave detectors, and offline analyses of the slow wave detector in the different conditions, and the percentages of tactile stimulation across sleep stages. ***A***, The leave-one-subject-out cross-validation confirmed that the artifact detector successfully classified EEG epochs as an artifact-contaminated EEG, and the slow wave detector classified EEG epochs as slow wave activity (artifact detector: $p < 10^{-6}$; slow wave detector: $p < 10^{-6}$; two-sided binomial test). ***B***, The AUC calculated by the receiver operating characteristic curve with the cross-validation of each detector confirmed that both detectors had sufficient accuracies (AUC of the artifact detector = 0.82 ± 0.0059 [mean ± SEM], AUC of the slow wave detector = 0.90 ± 0.0011). Dotted line indicates the baseline. ***C***, The offline analysis of the slow wave detection confirmed that the detector successfully classified EEG epochs as slow wave activities or no slow wave activities above chance level (SLEEP-MOTION condition: $p < 10^{-6}$ for all participants; SLEEP-RANDOM condition: $p < 10^{-6}$ for all participants; two-sided binomial test). ***D***, The percentages of tactile stimulation across sleep stages verified that the slow wave detector allowed for selective timing of tactile stimulation during Stage N3 sleep. *Post hoc* verification indicated that the classification results in Stage N2 were derived from the transition period between Stage N2 and N3, while the results in Stage W were derived from the sudden waking epochs immediately after Stage N3. Chance level is 50%. Error bars indicate SEM.

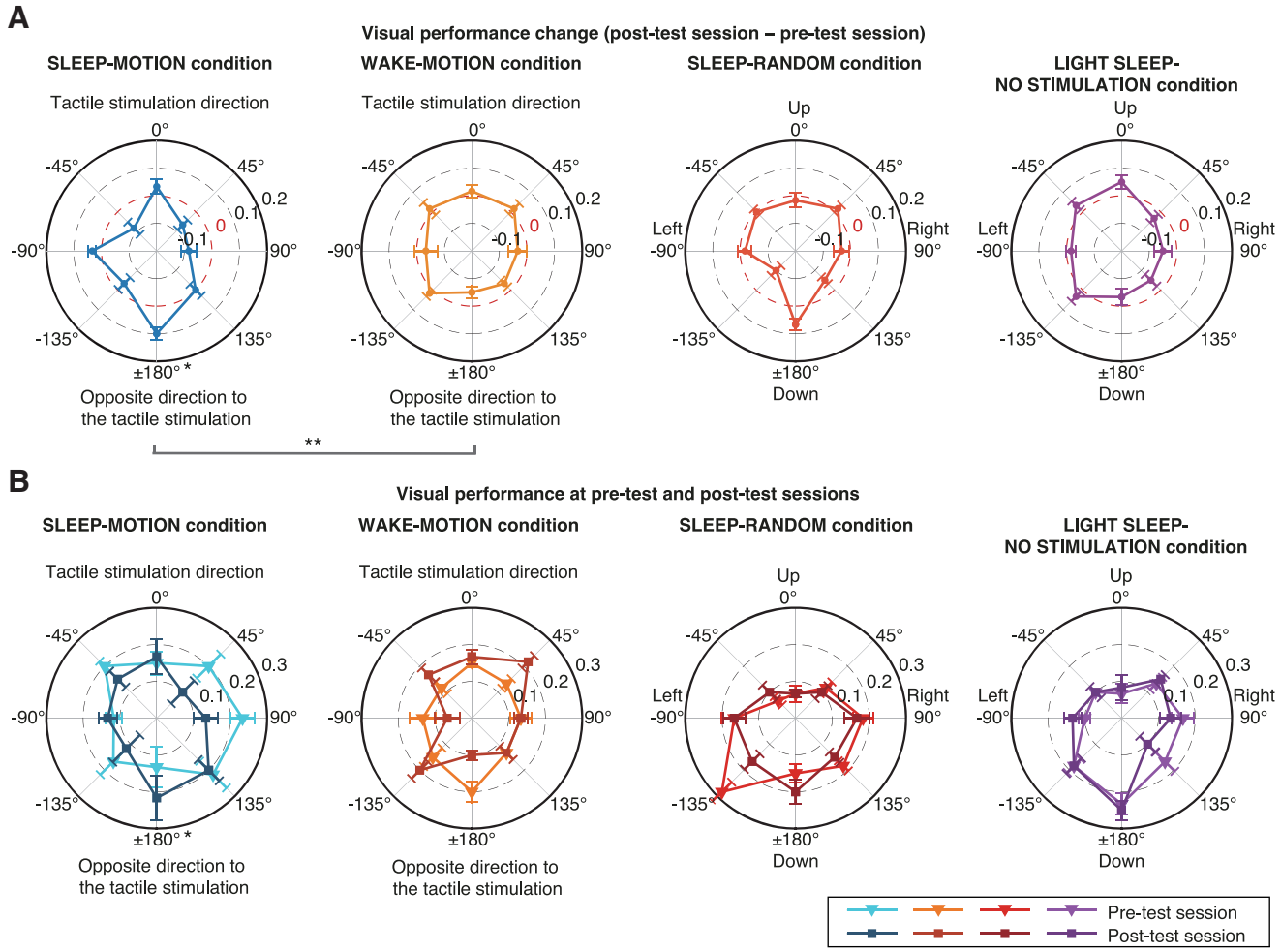

Figure 3. Behavioral performance of the random dot motion task. ***A***, Visual performance change in four conditions. The radial axis plots the difference of the correct ratio from the pre-test session to the post-test session. Each colored line indicates the median value of the difference of the correct ratio. The degrees in SLEEP-MOTION and WAKE-MOTION conditions indicate the angle of the visual coherent motion relative to the tactile motion direction based on the hand-centered reference frame. The degrees in SLEEP-RANDOM and LIGHT SLEEP-NO STIMULATION conditions indicate the angle of the visual coherent motion. ***B***, Correct ratio at the pre- and post-test sessions in four conditions. The radial axis plots the correct ratio. Error bar indicates SEM. $^{*}p < 0.05$. $^{**}p < 0.01$. This figure is extended in Extended Data Figures 3-1 and 3-2.

Table 1. The mean number of tactile stimulations, and mean interstimulus intervals of the tactile stimulations, the motion coherence threshold in the random dot motion task, the surface area of the index fingertip, the scores of Edinburgh Handedness Inventory, and sleep architecture (mean ± SEM) in Experiment 1

	No. of tactile stimulations	Mean interstimulus intervals	Motion coherence threshold (%)	Surface area (mm^2)	Hand score (points)
SLEEP-MOTION	238.4 ± 49.7	9.4 ± 2.1	7.8 ± 1.6	272.9 ± 11.9	91.0 ± 4.1
SLEEP-RANDOM	286.3 ± 73.7	9.8 ± 1.7	4.8 ± 0.6	266.9 ± 12.8	89.8 ± 3.6
LIGHT SLEEP-NO STIMULATION	NA	NA	5.0 ± 0.9	278.1 ± 12.3	86.4 ± 4.9
WAKE-MOTION	248.4 ± 3.1	6.2 ± 1.7	5.9 ± 0.9	281.1 ± 12.7	86.6 ± 4.3
p value (comparison across four conditions)	0.41	0.13	0.21	0.86	0.89

Sleep architecture

	Stage W (min)	Stage N1 (min)	Stage N2 (min)	Stage N3 (min)	Stage R (min)
SLEEP-MOTION	16.9 ± 4.0	8.7 ± 1.5	39.6 ± 2.6	24.0 ± 2.9	0 ± 0
SLEEP-RANDOM	13.3 ± 3.0	8.0 ± 2.6	36.8 ± 3.8	32.0 ± 4.2	0 ± 0
LIGHT SLEEP-NO STIMULATION	43.7 ± 7.0	14.8 ± 2.9	30.5 ± 6.9	0 ± 0	0 ± 0
WAKE-MOTION	NA	NA	NA	NA	NA
p value (SLEEP-MOTION vs. SLEEP-RANDOM)	0.49	0.82	0.59	0.11	NA

Detection methods and quantification of the spindles and slow waves

After applying a 0.2-4 Hz bandpass filter to the EEG potentials on each electrode, slow waves were identified when the EEG activity met three criteria that conformed to the sleep scoring manual (Iber et al., 2007). The slow wave density in Stages N2 and N3 was calculated as the number of slow waves per minute. For the slow, fast, and both types of spindle detection, all EEG potentials were processed by bandpass filtering of 11-13 Hz for slow spindles, 13-15 Hz for fast spindles, or 11-16 Hz for both types of spindles; and subsequently, the signal envelopes were computed by the Hilbert transform. Spindles were detected when the

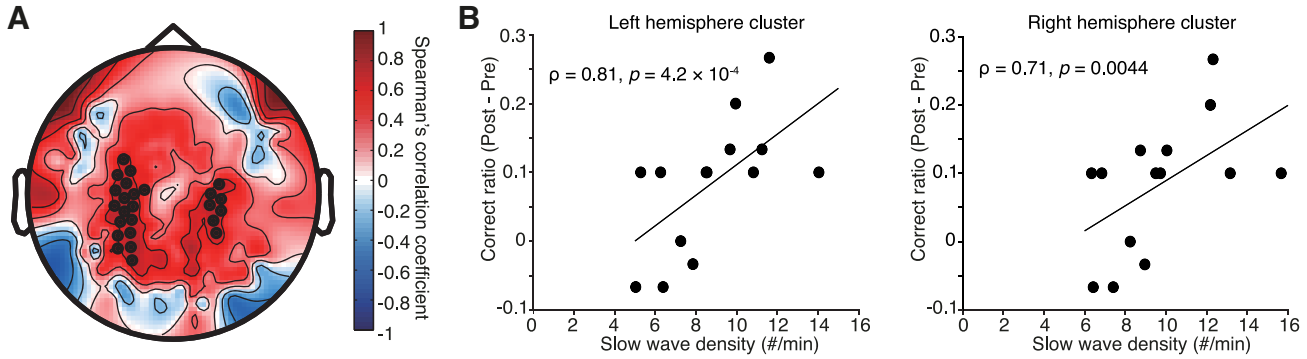

Figure 4. The correlation between the slow wave density in the sleep Stage N3 and the performance changes in the direction opposite to the tactile stimulation in the SLEEP-MOTION condition. ***A***, Topographic map of the correlation coefficients. Black dots represent significant electrodes in the clusters. ***B***, Correlation plot of the averaged slow wave density derived by electrodes in the clusters and the performance changes in the direction opposite to the tactile stimulation.

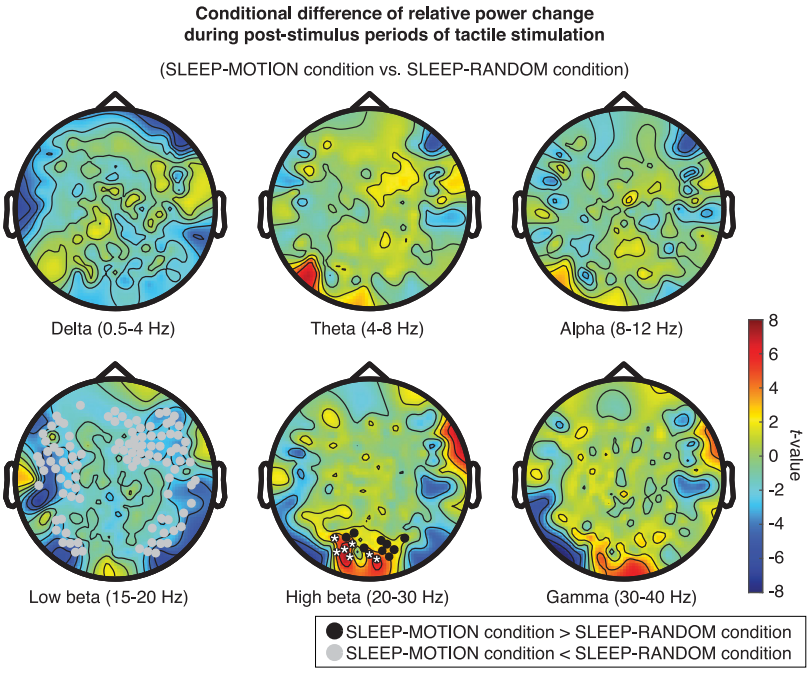

Figure 5. The topographic maps of the difference in relative power change during the post-stimulus periods between SLEEP-MOTION and SLEEP-RANDON conditions in sleep Stage N3. The topographic maps of the relative power difference between conditions in six frequency bands (delta, 0.5-4 Hz; theta, 4-8 Hz; alpha, 8-12 Hz; low beta, 15-20 Hz; high beta, 20-30 Hz; gamma, 30-40 Hz). Black and gray dots represent the positive and the negative electrode cluster, respectively, from the cluster-based permutation test. White asterisks in the high beta band represent the electrodes that showed the significant higher activations in SLEEP-MOTION condition ($p < 0.05$ adjusted by Bonferroni correction across electrodes).

envelope was above a 3 μV threshold. Spindle density in Stages N2 and N3 was calculated as the number of spindles per minute. The numbers and densities of spindles and slow waves in each sleep Stage N2 and N3 were computed at each electrode by using previously described methods for offline spindle and slow wave detection (Massimini et al., 2004; Piantoni et al., 2013).

The difference of the slow wave density and fast/slow spindle density between conditions was computed by two-tailed independent-sample *t* tests. To control for multiple comparisons across electrodes, we performed a cluster-based permutation test (Maris and Oostenveld, 2007) with 5000 iterations and a cluster-forming threshold of 0.05 with maxsum statistics based on the sum of *t* statistics, using Mass Univariate ERP Toolbox (Groppe et al., 2011). The α level for the cluster-wise *p* values ($p < 0.05$, two-tailed) was set to 0.017 (= 0.05/3 features) as adjusted by Bonferroni correction for the multiple comparisons of the three features (slow wave density, fast spindle density, and slow spindle density).

Time-frequency analysis of the post-stimulus period of the tactile stimulation

To assess the activation of the visual area induced by the tactile motion stimulation during sleep, we compared the spectral contents of the post-stimulus period between the motion and random tactile stimulation in slow wave sleep in the SLEEP-MOTION and SLEEP-RANDOM conditions. Since it takes 200 ms to achieve the motion sensation, we focused on the post-stimulus period from 200 to 300 ms. The total number of EEG epochs in Stage N3 was 2822 in SLEEP-MOTION condition and 3744 in SLEEP-RANDOM condition. The 256-channel EEG data were rereferenced by the average EEG data of the left and right mastoids, and bandpass filtered (0.5-40 Hz) after DC offset removal. EEG data were chunked as 1500 ms epochs that consist of 750 ms pre-stimulus period, 200 ms stimulus period, and 550 ms post-stimulus periods. EEG data with poor signal quality were excluded by visual inspection of the data. The power spectra were computed by fieldtrip toolbox (Oostenveld et al., 2011), adopting a Hanning taper method with a 500 ms fixed sliding window length. The average relative power change of the post-stimulus interval from 200 to 300 ms with respect to the pre-stimulus baseline interval from −300 to −100 ms was computed on each electrode in each frequency band (δ, 0.5-4 Hz; theta, 4-8 Hz; alpha, 8-12 Hz; low β, 15-20 Hz; high β, 20-30 Hz; γ, 30-40 Hz).

The difference of the power change subsequent to the tactile stimulation between conditions was evaluated by a two-tailed independent-sample *t* test in each frequency band. To control for multiple comparisons across electrodes, we performed a cluster-based permutation test with 5000 iterations and a cluster-forming threshold of 0.05 with maxsum statistics based on the sum of *t* statistics, using fieldtrip toolbox (Maris and Oostenveld, 2007; Oostenveld et al., 2011). The α level for the cluster-wise *p* values ($p < 0.05$, two-tailed) was set to 0.0083 (= 0.05/6 frequency bands) adjusted by Bonferroni correction for the multiple comparisons of the six frequency bands. When there was a significant conditional difference that showed higher activations in SLEEP-MOTION condition than in SLEEP-RANDOM condition at a specific frequency range, an additional parametric test, a two-tailed independent-sample *t* test with Bonferroni correction for multiple comparisons across all electrodes, was performed to evaluate the spatial extent of the conditional difference.

Post-experiment questionnaire and measurement of fingertip areas

The post-experiment questionnaire was provided to participants to assess the participants' awareness of the tactile stimulation and the

stimulation direction, and the hand preferences of participants. The hand preferences were evaluated by the modified version of the Edinburgh Handedness Inventory (Oldfield, 1971). Afterward, to measure the anterior area of the right index fingertip, the index fingers were scanned at 1200 dpi by a digital scanner (HP Scanjet G4010, Hewlett-Packard Development). The image of the anterior area of the index fingertip was segmented manually and converted into binary images by the global image threshold. Subsequently, the area was calculated as the number of pixels and converted from pixels to mm^2. All calculations were performed using MATLAB Image Processing Toolbox (The MathWorks).

Statistical analyses

All statistical analyses were computed with IBM SPSS Statistics (SPSS version 22L) and MATLAB (R2011b, The MathWorks).

Behavior indices. The correct ratio of visual motion discrimination was calculated in each pre-test and post-test session. The changes of the correct ratio served as the effect of primary interest and were calculated by subtracting the performance of the pre-test session from the performance of the post-test session for all eight directions. To validate the behavioral improvement, we adopted a two-tailed Wilcoxon signed-rank test adjusted by Bonferroni correction to the performance changes between pre- and post-test sessions at eight visual motion directions in all conditions. To compare behavioral performances between SLEEP-MOTION and WAKE-MOTION conditions, two-tailed two-sample Mann–Whitney's *U* tests adjusted by Bonferroni correction for multiple comparisons were applied. In addition, two separate permutation tests were performed with 10^5 iterations to test whether median values of the visual performance change in the SLEEP-RANDOM and LIGHT SLEEP-NO STIMULATION conditions exceeded the median values of the visual performance change at the opposite direction to the tactile motion stimulation in the SLEEP-MOTION condition. In the permutation test, the performance change data of eight directions in either SLEEP-RANDOM or LIGHT SLEEP-NO STIMULATION condition was shuffled in random order within each participant. Subsequently, the *p* value was calculated, comparing the performance change at the opposite direction of the tactile motion stimulation in the SLEEP-MOTION condition against the distribution of the performance change from the randomized data.

To examine the association between behavioral improvements and sleep physiological factors, Spearman's rank correlation coefficient was calculated to assess associations between the performance changes of the opposite direction to the tactile motion stimulation in the SLEEP-MOTION condition and the slow wave density and fast/slow spindle density of Stage N3 across all electrodes. To control for multiple comparisons across electrodes, we performed a cluster-based permutation test (Maris and Oostenveld, 2007) with 5000 iterations and a cluster-forming threshold of 0.05 with maxsum statistics based on the sum of *t* statistics, using a modified script of Mass Univariate ERP Toolbox (Groppe et al., 2011) used in the previous study (Baranauskas et al., 2017) that allowed us to compute Spearman's rank correlation coefficient instead of Pearson correlation coefficient. The α level for the cluster-wise *p* values ($p < 0.05$, two-tailed) was set to 0.0063 (= 0.05/8 directions) adjusted by Bonferroni correction for the multiple comparisons of the possible eight motion directions.

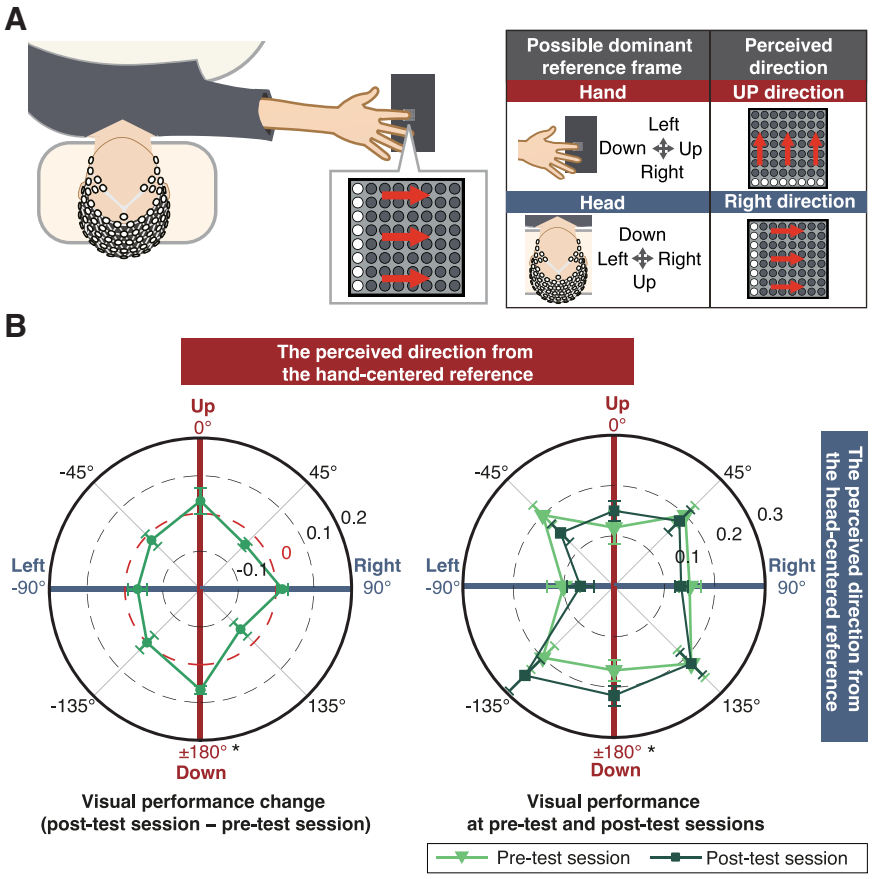

Figure 6. The experimental setup of Experiment 2 and visual performance. ***A***, The schematic diagram of the experimental setup and the expected outcomes from the possible dominant reference frames: hand-centered reference frame and head-centered reference frame. ***B***, Visual performance change and correct ratio at pre- and post-test sessions in Experiment 2. Left, Green line indicates the median value of the difference of the correct ratio. Right, Each green and light green line indicates the correct ratio at the pre- and post-test sessions. The degrees indicate the angle of the visual coherent motion. Error bar indicates SEM. $*p < 0.05$.

Physiologic indices. Two-tailed one-way ANOVA was conducted to compare the threshold of the visible motion coherence level between conditions, the scores of Edinburgh Handedness Inventory, the difference of the number of tactile stimulations and mean inter-stimulus intervals between experimental conditions, and the differences in the surface area of fingertips between the four conditions. To compare durations of each sleep stage between SLEEP-MOTION and SLEEP-RANDOM conditions and between SLEEP-MOTION and SLEEP-POSTURE conditions, a two-tailed two-sample *t* test was performed.

Data availability

Further information and requests for all data relevant to the conclusion of this paper are available from the corresponding authors on reasonable request.

Results

Tactile stimulation during sleep biases the post-sleep visual improvement in a direction-selective manner

We examined the performance changes of the visual motion detection across periods of sleep and wakefulness. For the analysis, we postulated that the visual motion direction was congruent with the tactile motion direction defined by the hand-centered reference frame (i.e., the up-motion direction on the fingertip corresponds to the up-motion direction on the visual area). The performance changes of participants that received tactile motion

stimulation across sleep and wake in SLEEP-MOTION and WAKE-MOTION conditions showed a significant difference between conditions only in the direction opposite to the tactile motion stimulation during slow wave sleep ($p = 0.0064$, $Z = 3.40$, effect size $r = 0.64$; two-tailed two-sample Mann–Whitney's U test adjusted by Bonferroni correction for multiple comparisons; Fig. 3*A*). Additionally, a significant improvement of the performance change between pre-test and post-test sessions across sleep occurred only in the direction opposite to the tactile motion stimulation ($p = 0.04$, $Z = 2.79$, effect size $r = 0.53$; two-tailed Wilcoxon signed-rank test adjusted by Bonferroni correction for multiple comparisons; Fig. 3*A,B*). In contrast, no improvement in any direction occurred when participants received the tactile stimulation during waking. Furthermore, participants in the SLEEP-RANDOM and LIGHT SLEEP–NO STIMULATION conditions showed no visual improvement in any direction (all $p > 0.05$; two-tailed Wilcoxon signed-rank test adjusted by Bonferroni correction for multiple comparisons). To compare the behavioral improvement found in SLEEP-MOTION condition with the two other control conditions, we also performed a permutation test by comparing the shuffled performance changes in SLEEP-RANDOM and LIGHT SLEEP-NO STIMULATION conditions with the performance change in SLEEP-MOTION conditions at the opposite target direction. As a result, there was no significant difference between these conditions ($p > 0.9998$). No conditional difference was found with respect to thresholds of dot motion coherence for the task ($F_{(3,52)} = 1.57$, $p = 0.21$, two-tailed one-way ANOVA), the duration of sleep stages, the number of tactile stimulations ($F_{(2,39)} = 0.91$, $p = 0.41$, two-tailed one-way ANOVA), or the mean interstimulus intervals ($F_{(2,39)} = 2.18$, $p = 0.13$, two-tailed one-way ANOVA) (Table 1). In both conditions, >85% of the stimulation was presented in sleep Stage N3. These results suggest that tactile motion information during slow wave sleep induces a direction-selective facilitation of the visual performance after sleep, possibly based on the hand-centered reference frame.

To investigate sleep factors that account for individual differences in the sleep-dependent visual improvement at the direction opposite to tactile motion stimulation in SLEEP-MOTION condition, we performed a correlation analysis of the cross-sleep motion improvement and the slow wave density and fast/slow spindle density detected at each EEG electrode in sleep Stage N3. We found a significant association of Stage N3 slow wave density with the enhancement of the visual motion detection (left hemisphere cluster $t = 48.42$, right hemisphere cluster $t = 22.67$, $p < 0.0063$; Fig. 4*A*). Highly correlated electrodes ($\rho > 0.7$) included significant electrodes forming clusters found over bilateral parietal areas. The correlation coefficient between the visual improvement and the averaged slow wave density of electrodes within the cluster was 0.81 (left hemisphere cluster) and 0.71 (right hemisphere cluster) (Fig. 4*B*). No significant correlation was found for the fast/slow spindle density. These results suggest that the ongoing slow wave activity possibly provides a suitable state for the consolidation of neural adaptation by repeated tactile stimulation.

To assess whether the tactile motion stimulation activates the visual regions of the sleeping brain in agreement with previous reports during the waking state (Zangaladze et al., 1999; Hagen et al., 2002; Müller et al., 2019), we performed a time-frequency analysis to compute EEG power spectra during the post-stimulus periods of every tactile motion stimulation and tactile random stimulation in sleep Stage N3. We compared the relative power change of the post-stimulus periods between these two different tactile stimulations in multiple frequency bands (delta, 0.5-4 Hz; theta, 4-8 Hz; alpha, 8-12 Hz; low beta, 15-20 Hz; high beta, 20-30 Hz; gamma, 30-40 Hz). The results showed that linear tactile motion stimulation presented in the SLEEP-MOTION condition induced a significantly higher power in the high beta frequency band (20-30 Hz) than tactile random stimulation presented in the SLEEP-RANDOM condition (cluster $t = 65.23$, $p < 0.0083$; Fig. 5). The conditional difference was prominent over the occipital electrodes possibly overlying the visual area ($p < 0.05$ adjusted by Bonferroni correction for multiple comparison across electrodes). In contrast, the activation during the tactile motion stimulation was significantly lower at the low beta frequency. Since the motion and random stimulation conditions were matched for spatial-temporal features of the stimulation, except the motion aspect, this suggests that the high beta frequency reflects visual cortical processing of tactile motion information during sleep while the low beta frequency may reflect sensory processing, which may account for a stronger sensation in the random tactile stimulation than the linear tactile stimulation. This finding confirmed that the repetitive tactile motion stimulation induced high activations in the occipital electrodes overlying the visual regions during sleep.

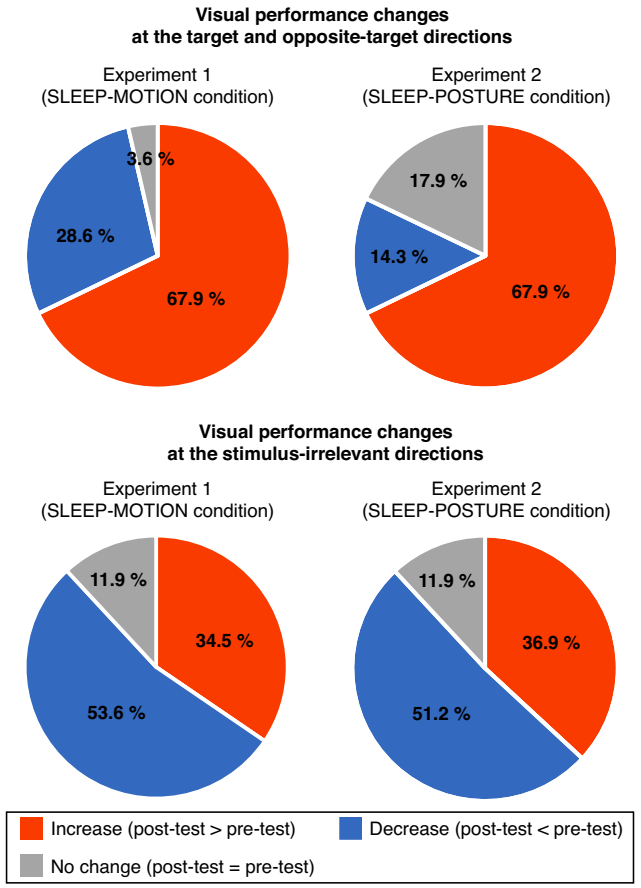

Figure 7. The ratio of the visual performance changes (post-test – pre-test) in SLEEP-MOTION and SLEEP-POSTURE conditions. The visual performance changes at the target and opposite-target directions are mostly increased, whereas stimulus-irrelevant directions (i.e., all directions except target direction and opposite target direction) are mostly decreased or not changed.

Hand-centered reference frame plays a dominant role to determine tactile motion direction during sleep for post-sleep visual improvement

Our results from the first experiment suggest that repetitive tactile information during sleep induced the biased facilitation of the visual performance in a direction-selective manner. It implies that the hand-centered reference frame was possibly dominant to determine the tactile motion direction that influenced the sleep-dependent visual improvement. However, it remains unclear whether the other body reference frame, especially the head-centered reference frame, may influence this visual improvement and how body reference frames were selected during sleep in the misalignment situation of body references to judge tactile motion direction for the selective post-sleep enhancement of visual motion detection. Therefore, we conducted a second experiment that misaligns the hand- and head-centered reference frames by manipulating limb posture. The experimental setup and stimulus parameters were the same as the first experiment. We induced the tactile linear motion from the bottom row to the top row on the index fingers of the new participants whose right arms were stretched out at 90 degrees to the side (SLEEP-POSTURE condition) (Fig. 6*A*). The linear motion can be recognized either as a vertical direction from the hand-centered reference frame or a horizontal direction from the head-centered reference frame.

In the behavioral performance, the visual improvement was found only on the orientation of the hand-centered reference frame, especially in the vertical "down" direction ($p = 0.024$, $Z = 3.00$, effect size $r = 0.57$; two-tailed Wilcoxon signed-rank test adjusted by Bonferroni correction for multiple comparisons. Fig. 6*B*). No visual improvement was observed in any direction. Similar to the results of the SLEEP-MOTION condition, the results of the SLEEP-POSTURE condition showed that the visual improvement was dominant at the stimulus-related directions while the visual performance changes at the stimulus-irrelevant motion directions were mostly decreased or not changed (Fig. 7).

Regarding EEG characteristics of the SLEEP-POSTURE condition, the analysis of the spatial distribution of slow wave density and fast/slow spindle density during sleep Stage N3 revealed broadly suppressed slow wave activity (cluster $t = -362.39$, $p < 0.017$) and increased fast spindle activity (cluster $t = 755.10$, $p < 0.017$) in the SLEEP-POSTURE condition, compared with the SLEEP-MOTION condition of the Experiment 1 (Fig. 8). No conditional difference was found in the duration of sleep stages (Table 2).

These results suggest that the hand-centered reference frame becomes dominant during sleep, even in the misalignment situation across the multiple reference frames for the tactile motion coordination, which determines direction-selective enhancement of visual motion detection.

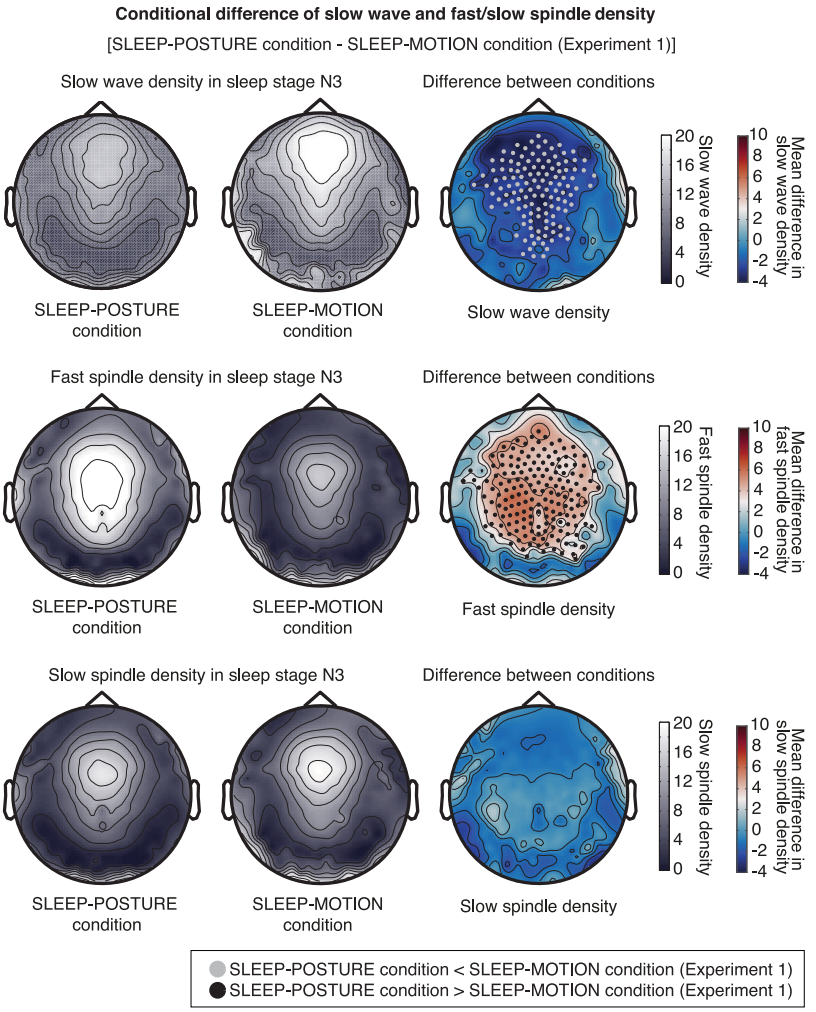

Figure 8. A topographical visualization of the significant difference of slow wave density and fast spindle density in sleep Stage 3 between SLEEP-POSTURE condition and SLEEP-MOTION condition (Experiment 1). Gray and black dots represent the negative and positive electrode clusters, respectively.

Discussion

Using the closed-loop interface that automatically delivered tactile motion stimulation triggered by slow wave activity mainly in sleep Stage N3, we observed selective post-sleep improvement of visual motion detection exclusively in the direction opposite to the tactile motion stimulation. The visual improvement was positively associated with slow wave density. The tactile linear motion stimulation induced higher activation specifically over the occipital region in the high beta frequency (20-30 Hz). For the achievement of visual-tactile interaction during sleep, the hand-centered reference frame dominates to anchor the coordination of the tactile motion direction during sleep, even under misalignment of multiple body reference frames.

Our results reveal, for the first time, that visual-tactile cross-modal interaction as a form of motion adaptation can occur during sleep. The findings are in agreement with the report that repetitive sound stimulation induces a stimulus-specific adaptation during both non-rapid and rapid eye movement sleep (Nir et al., 2015) and commensurate with previous work showing an opposite visual motion aftereffect after directional tactile stimulation during wakefulness (Konkle et al., 2009; Xiao et al., 2021). The neural mechanism of the motion aftereffect is thought to involve a selective neural adaptation resulting in an imbalance between

Table 2. The mean number of tactile stimulations, and mean interstimulus intervals of the tactile stimulations, the motion coherence threshold in the random dot motion task, the surface area of the index fingertip, the scores of Edinburgh Handedness Inventory, and sleep architecture (mean ± SEM) in Experiment 2

	No. of tactile stimulations	Mean interstimulus intervals	Motion coherence threshold (%)	Surface area (mm^2)	Hand score (points)
SLEEP-POSTURE	131.2 ± 36.7	8.7 ± 1.9	10.4 ± 1.6	264.1 ± 5.1	83.8 ± 6.3
p values (SLEEP-POSTURE vs. SLEEP-MOTION)	0.076	0.73	0.21	0.55	0.38

Sleep architecture

	Stage W (min)	Stage N1 (min)	Stage N2 (min)	Stage N3 (min)	Stage R (min)
SLEEP-POSTURE	14.1 ± 2.8	6.6 ± 1.5	37.5 ± 3.1	28.4 ± 2.9	0 ± 0
p values (SLEEP-POSTURE vs. SLEEP-MOTION)	0.60	0.41	0.71	0.25	NA

the activities of subpopulations of different direction-selective neurons in both visual and tactile motion-processing areas, such as visual cortical area (V1-V3) and hMT/V5 (Mather et al., 2008). Furthermore, complementing cross-modal fMRI studies (Zangaladze et al., 1999; Hagen et al., 2002), our time-frequency analysis reveals that tactile motion stimulation induces a higher activation in occipital electrodes over the visual areas in the high beta frequency (20-30 Hz). The beta frequency band (14-30 Hz) has been reported to reflect sensorimotor processing (Brovelli et al., 2004), and tactile stimulation induced stronger effective connectivity of the beta frequency band from both somatosensory cortex and visual cortex to thalamus, in comparison between the sighted group and a congenitally blind group (Müller et al., 2019). It suggests a functional interaction of neuronal ensembles for the motion information processing across different sensory circuits during sleep through the thalamocortical system (McCormick and Bal, 1994) that underlies sensory adaptation (Mease et al., 2014).

Why does the cross-modal motion adaptation during sleep facilitate the post-sleep visual performance? We further found that the visual improvement subsequent to the repetitive tactile motion stimulation during sleep was associated with the slow wave activity over the bilateral parietal electrodes possibly corresponding to the somatosensory areas in sleep Stage N3. Slow wave activity has been known to be modulated by external sensory stimuli to enhance memory performance (Ngo et al., 2013). Together with the aforementioned neural adaptation process, our results suggest that (1) a selective imbalance of synaptic connections for visual motion processing by tactile motion stimulation forms the visual-tactile motion adaptation possibly through the thalamocortical system, and (2) the repeated neural patterns of the visual-tactile motion adaptation facilitate the synaptic strength of the neural populations for the opposite target motion detection through the sleep-dependent consolidation process by slow wave activity, which results in a selective visual improvement after sleep. This neural mechanism of the sleep-dependent consolidation process may be explained by either the reactivation model (Oudiette and Paller, 2013; Wilckens et al., 2018; Klinzing et al., 2019; Simor et al., 2020) or the synaptic homeostasis model (Tononi and Cirelli, 2014). In addition to the selective enhancement of the post-sleep visual performance, we observed the suppression of the visual performance at the stimulus-irrelevant motion directions (Fig. 7). It may be associated with the sleep-dependent selective-downscaling of task-irrelevant neural populations reported in the sleep study of neuroprosthetic learning (Gulati et al., 2017). Further research is necessary to examine a possible mechanism of the sleep-dependent consolidation and the down-selection process.

In addition to our finding of Experiment 1, our results from Experiment 2 suggest maintenance of a body spatial reference frame, the hand-centered reference frame, during sleep that fosters a contribution to the sleep-dependent visual improvement. In contrast to the SLEEP-MOTION condition of Experiment 1, we found a decreased slow wave density and increased fast spindle density over the frontal and parietal electrodes during sleep Stage N3 in the SLEEP-POSTURE condition (Fig. 8). Similar to a previous study (Dang-Vu et al., 2010), it may reflect that sleep spindles function to maintain sleep, while keeping an unusual body posture decreases the slow wave density. In addition, since fast spindles have also been known to be associated with sleep-dependent visuomotor performance (Tamaki et al., 2008; Peyrache and Seibt, 2020), this may reflect the interpretation of the tactile motion direction and the selection process of the reference frame.

A possible cause to prioritize hand-centered reference frames during sleep may be attributed to a lower corticocortical connectivity in the slow wave periods (Massimini et al., 2005; Tagliazucchi and Laufs, 2014). For the tactile spatial processing, tactile information from the skin/hand (the primary source of the tactile sensation) would then convert into other body reference frames based on the integration of weights assigned to each reference frame for the judgment of tactile spatial location (Heed et al., 2015). The lower corticocortical connectivity might induce lower information weights of reference frames than the hand-centered reference frame, which would then have resulted in the preservation of the primary coordinate system of the tactile motion direction. Since all previous studies were conducted in the awake state, however, further exploration is required to understand the underlying neural mechanisms of the body reference for tactile perception during sleep.

There are several limitations to be mentioned in this study. First, there is a possibility that not only the 30-40 min pre-test session but also the 15 min assessment session, being almost half the duration of the pre-test session, may contribute to visual training before sleep. Further study may be necessary to find whether the cross-modal selective enhancement can be achieved without the visual training session before sleep. Second, to evaluate the effect of the tactile motion stimulation during sleep, we compared the visual performance change in SLEEP-MOTION and WAKE-MOTION conditions (Fig. 3). In addition to the conditional difference of sleep and wake status, the difference of the body posture, the supine body in sleep condition, and upright body posture in wake condition may change the alertness on the tactile motion stimulation. Although no improvement at a specific visual motion direction was found in the WAKE-MOTION condition, which indicates that the difference alertness may not influence the improvement of the visual motion detection, further study is needed to perform the subthreshold tactile stimulation, such as electrocutaneous stimulation (Ramos-Estebanez et

al., 2007), which minimizes the tactile alertness in both sleep and wake conditions. In addition to the aforementioned limitation, we demonstrated that the post-sleep visual improvement occurs through a visual-tactile cross-modal motion adaptation during a daytime nap. Although sleep has been known to contribute on the long-term stabilization of the enhanced visual sensitivity through the consolidation as seen in studies of visual perceptual learning (Stickgold et al., 2000), further investigation is needed to elucidate whether the improvement of the visual motion detection in our study will be sustained for a long period.

Previous studies have coupled multimodal sensory stimuli before sleep for the subsequent targeted memory reactivation during sleep to induce selective memory enhancement (Rasch et al., 2007; Rudoy et al., 2009). The targeted memory reactivation paradigms have been adopted for the association memory formation of unrelated information, such as visual object locations, sound, and odor. However, we demonstrated the induction of a selective enhancement of the visual performance through a cross-modal interaction of novel tactile information provided during sleep. Together, we here show that nonassociated sensory information can induce the post-sleep selective enhancement of the visual performance when an anatomic and functional neural association is inherently established between these sensory modalities.

References

Antony JW, Gobel EW, O'Hare JK, Reber PJ, Paller KA (2012) Cued memory reactivation during sleep influences skill learning. Nat Neurosci 15:1114–1116.

Azañón E, Soto-Faraco S (2008) Changing reference frames during the encoding of tactile events. Curr Biol 18:1044–1049.

Baranauskas M, Grabauskaitė A, Griškova-Bulanova I (2017) Brain responses and self-reported indices of interoception: heartbeat evoked potentials are inversely associated with worrying about body sensations. Physiol Behav 180:1–7.

Bensmaïa SJ, Killebrew JH, Craig JC (2006) Influence of visual motion on tactile motion perception. J Neurophysiol 96:1625–1637.

Brainard DH (1997) The Psychophysics Toolbox. Spat Vis 10:433–436.

Brovelli A, Ding M, Ledberg A, Chen Y, Nakamura R, Bressler SL (2004) Beta oscillations in a large-scale sensorimotor cortical network: directional influences revealed by Granger causality. Proc Natl Acad Sci USA 101:9849–9854.

Buysse DJ, Reynolds CF, Monk TH, Berman SR, Kupfer DJ (1989) The Pittsburgh Sleep Quality Index: a new instrument for psychiatric practice and research. Psychiatry Res 28:193–213.

Carney CE, Buysse DJ, Ancoli-Israel S, Edinger JD, Krystal AD, Lichstein KL, Morin CM (2012) The consensus sleep diary: standardizing prospective sleep self-monitoring. Sleep 35:287–302.

Carter O, Konkle T, Wang Q, Hayward V, Moore C (2008) Tactile rivalry demonstrated with an ambiguous apparent-motion quartet. Curr Biol 18:1050–1054.

Chang CC, Lin CJ (2011) LIBSVM: a library for support vector machines. ACM Trans Intell Syst Technol 2:1–27.

Chang PP, Ford DE, Mead LA, Cooper-Patrick L, Klag MJ (1997) Insomnia in young men and subsequent depression: the Johns Hopkins Precursors Study. Am J Epidemiol 146:105–114.

Dang-Vu TT, McKinney SM, Buxton OM, Solet JM, Ellenbogen JM (2010) Spontaneous brain rhythms predict sleep stability in the face of noise. Curr Biol 20:R626–R627.

Groppe DM, Urbach TP, Kutas M (2011) Mass univariate analysis of event-related brain potentials/fields: I. A critical tutorial review. Psychophysiology 48:1711–1725.

Gulati T, Guo L, Ramanathan DS, Bodepudi A, Ganguly K (2017) Neural reactivations during sleep determine network credit assignment. Nat Neurosci 20:1277–1224.

Hagen MC, Franzén O, McGlone F, Essick G, Dancer C, Pardo JV (2002) Tactile motion activates the human middle temporal/V5 (MT/V5) complex. Eur J Neurosci 16:957–964.

Heed T, Buchholz VN, Engel AK, Röder B (2015) Tactile remapping: from coordinate transformation to integration in sensorimotor processing. Trends Cogn Sci 19:251–258.

Iber C, Ancoli-Israel S, Chesson A, Quan S (2007) The AASM Manual for the Scoring of Sleep and Associates Events: rules, terminology and technical specifications. American Academy of Sleep Medicine.

Klinzing JG, Niethard N, Born J (2019) Mechanisms of systems memory consolidation during sleep. Nat Neurosci 22:1598–1610.

Konkle T, Wang Q, Hayward V, Moore CI (2009) Motion aftereffects transfer between touch and vision. Curr Biol 19:745–750.

Maris E, Oostenveld R (2007) Nonparametric statistical testing of EEG- and MEG-data. J Neurosci Methods 164:177–190.

Mascetti L, Muto V, Matarazzo L, Foret A, Ziegler E, Albouy G, Sterpenich V, Schmidt C, Degueldre C, Leclercq Y, Phillips C, Luxen A, Vandewalle G, Vogels R, Maquet P, Balteau E (2013) The impact of visual perceptual learning on sleep and local slow wave initiation. J Neurosci 33:3323–3331.

Massimini M, Huber R, Ferrarelli F, Hill S, Tononi G (2004) The sleep slow oscillation as a traveling wave. J Neurosci 24:6862–6870.

Massimini M, Ferrarelli F, Huber R, Esser SK, Singh H, Tononi G (2005) Breakdown of cortical effective connectivity during sleep. Science 309:2228–2232.

Mather G, Pavan A, Campana G, Casco C (2008) The motion aftereffect reloaded. Trends Cogn Sci 12:481–487.

McCormick DA, Bal T (1994) Sensory gating mechanisms of the thalamus. Curr Opin Neurobiol 4:550–556.

Mease RA, Krieger P, Groh A (2014) Cortical control of adaptation and sensory relay mode in the thalamus. Proc Natl Acad Sci USA 111:6798–6803.

Mednick S, Nakayama K, Stickgold R (2003) Sleep-dependent learning: a nap is as good as a night. Nat Neurosci 6:697–698.

Moscatelli A, Hayward V, Wexler M, Ernst MO (2015) Illusory tactile motion perception: an analog of the visual Filehne illusion. Sci Rep 5:14584.

Müller F, Niso G, Samiee S, Ptito M, Baillet S, Kupers R (2019) A thalamocortical pathway for fast rerouting of tactile information to occipital cortex in congenital blindness. Nat Commun 10:5154.

Ngo HV, Martinetz T, Born J, Mölle M (2013) Auditory closed-loop stimulation of the sleep slow oscillation enhances memory. Neuron 78:545–553.

Nir Y, Vyazovskiy VV, Cirelli C, Banks MI, Tononi G (2015) Auditory responses and stimulus-specific adaptation in rat auditory cortex are preserved across NREM and REM sleep. Cereb Cortex 25:1362–1378.

Oldfield RC (1971) The assessment and analysis of handedness: the Edinburgh inventory. Neuropsychologia 9:97–113.

Oostenveld R, Fries P, Maris E, Schoffelen JM (2011) FieldTrip: open source software for advanced analysis of MEG, EEG, and invasive electrophysiological data. Comput Intell Neurosci 2011:156869.

Oudiette D, Paller KA (2013) Upgrading the sleeping brain with targeted memory reactivation. Trends Cogn Sci 17:142–149.

Pei YC, Hsiao SS, Craig JC, Bensmaia SJ (2010) Shape invariant coding of motion direction in somatosensory cortex. PLoS Biol 8:e1000305.

Pei YC, Bensmaia SJ (2014) The neural basis of tactile motion perception. J Neurophysiol 112:3023–3032.

Peyrache A, Seibt J (2020) A mechanism for learning with sleep spindles. Philos Trans R Soc Lond B Biol Sci 375:22–24.

Piantoni G, Poil SS, Linkenkaer-Hansen K, Verweij IM, Ramautar JR, Van Someren EJ, Van Der Werf YD (2013) Individual differences in white matter diffusion affect sleep oscillations. J Neurosci 33:227–233.

Ramos-Estebanez C, Merabet LB, Machii K, Fregni F, Thut G, Wagner TA, Romei V, Amedi A, Pascual-Leone A (2007) Visual phosphene perception modulated by subthreshold crossmodal sensory stimulation. J Neurosci 27:4178–4181.

Rasch B, Büchel C, Gais S, Born J (2007) Odor cues during slow wave sleep prompt declarative memory consolidation. Science 315:1426–1429.

Rudoy JD, Voss JL, Westerberg CE, Paller KA (2009) Strengthening individual memories by reactivating them during sleep. Science 326:1079.

Sasaki Y, Nanez JE, Watanabe T (2010) Advances in visual perceptual learning and plasticity. Nat Rev Neurosci 11:53–60.

Schalk G, McFarland DJ, Hinterberger T, Birbaumer N, Wolpaw JR (2004) BCI2000: a general-purpose brain-computer interface (BCI) system. IEEE Trans Biomed Eng 51:1034–1043.

Shadlen MN, Newsome WT (1996) Motion perception: seeing and deciding. Proc Natl Acad Sci USA 93:628–633.

Simor P, van der Wijk G, Nobili L, Peigneux P (2020) The microstructure of REM sleep: why phasic and tonic? Sleep Med Rev 52:101305.

Soldatos CR, Dikeos DG, Paparrigopoulos TJ (2000) Athens Insomnia Scale: validation of an instrument based on ICD-10 criteria. J Psychosom Res 48:555–560.

Stickgold R, James L, Hobson J (2000) Visual discrimination learning requires sleep after training. Nat Neurosci 3:1237–1238.

Tagliazucchi E, Laufs H (2014) Decoding wakefulness levels from typical fMRI resting-state data reveals reliable drifts between wakefulness and sleep. Neuron 82:695–708.

Tamaki M, Matsuoka T, Nittono H, Hori T (2008) Fast sleep spindle (13-15 Hz) activity correlates with sleep-dependent improvement in visuomotor performance. Sleep 31:204–211.

Tononi G, Cirelli C (2014) Sleep and the price of plasticity: from synaptic and cellular homeostasis to memory consolidation and integration. Neuron 81:12–34.

Watanabe T, Náñez JE, Sasaki Y (2001) Perceptual learning without perception. Nature 413:844–848.

Wilckens KA, Ferrarelli F, Walker MP, Buysse DJ (2018) Slow wave activity enhancement to improve cognition. Trends Neurosci 41:470–482.

Xiao K, Gao Y, Imran SA, Chowdhury S, Commuri S, Jiang F (2021) Cross-modal motion aftereffects transfer between vision and touch in early deaf adults. Sci Rep 11:12.

Yotsumoto Y, Sasaki Y, Chan P, Vasios CE, Bonmassar G, Ito N, Náñez JE, Shimojo S, Watanabe T (2009) Location-specific cortical activation changes during sleep after training for perceptual learning. Curr Biol 19:1278–1282.

Zangaladze A, Epstein CM, Grafton ST, Sathian K (1999) Involvement of visual cortex in tactile discrimination of orientation. Nature 401:587–590.